

# TbVps34, the Trypanosome Orthologue of Vps34, Is Required for Golgi Complex Segregation<sup>\*S</sup>

Received for publication, March 8, 2006, and in revised form, July 10, 2006 Published, JBC Papers in Press, July 11, 2006, DOI 10.1074/jbc.M602183200

Belinda S. Hall<sup>†1</sup>, Carme Gabernet-Castello<sup>§</sup>, Andrew Voak<sup>‡</sup>, David Goulding<sup>‡</sup>, Senthil Kumar Natesan<sup>§</sup>, and Mark C. Field<sup>†S2</sup>

From the <sup>†</sup>Department of Biological Sciences, Imperial College of Science, Technology and Medicine, London SW7 2AY and the <sup>§</sup>Department of Pathology, University of Cambridge, Tennis Court Road, Cambridge CB2 1QP, United Kingdom

Phosphoinositides are important regulators of numerous cellular functions. The yeast class III phosphatidylinositol 3-kinase Vps34p, and its human orthologue hVPS34, are implicated in control of several key pathways, including endosome to lysosome transport, retrograde endosome to Golgi traffic, multivesicular body formation, and autophagy. We have identified the Vps34p orthologue in the African trypanosome, TbVps34. Knockdown of TbVps34 expression by RNA interference induces a severe growth defect, with a post-mitotic block to cytokinesis accompanied by a variety of morphological abnormalities. GFP2xFYVE, a chimeric protein that specifically binds phosphatidylinositol 3-phosphate, localizes to the trypanosome endosomal system and is delocalized under TbVps34 RNA interference (RNAi), confirming that TbVps34 is an authentic phosphatidylinositol 3-kinase. Expression of GFP2xFYVE enhances the TbVps34 RNAi-associated growth defect, suggesting a synthetic interaction via competition for phosphatidylinositol 3-phosphate-binding sites with endogenous FYVE domain proteins. Endocytosis of a fluid phase marker is unaffected by TbVps34 RNAi, but receptor-mediated endocytosis of transferrin and transport of concanavalin A to the lysosome are both impaired, confirming a role in membranous endocytic trafficking for TbVps34. TbVps34 knockdown inhibits export of variant surface glycoprotein, indicating a function in exocytic transport. Ultrastructural analysis revealed a highly extended Golgi apparatus following TbVps34 RNAi, whereas expression of the Golgi marker red fluorescent protein-GRASP (Grp1 (general receptor for phosphoinositides-1)-associated scaffold protein) demonstrated that trypanosomes are able to duplicate the Golgi complex but failed to complete segregation during mitosis, despite faithful replication and segregation of basal bodies and the kinetoplast. These observations implicate TbVps34 as having a role in coordinating segregation of the Golgi complex at cell division.

\* This work was supported by program grant funding from the Wellcome Trust (to M. C. F.). The costs of publication of this article were defrayed in part by the payment of page charges. This article must therefore be hereby marked "advertisement" in accordance with 18 U.S.C. Section 1734 solely to indicate this fact.

<sup>S</sup> The on-line version of this article (available at <http://www.jbc.org>) contains supplemental Table S1 and Figs. S1–S3.

<sup>1</sup> Present address: Neuromuscular Unit, Imperial College, London, W10 0NN, United Kingdom.

<sup>2</sup> To whom correspondence should be addressed: Dept. of Pathology, University of Cambridge, Tennis Court Road, Cambridge CB2 1QP, United Kingdom. Tel.: 44-1223-333734; E-mail: mcf34@cam.ac.uk.

Phosphatidylinositol (PI)<sup>3</sup> is a relatively minor component of lipid membranes in most cells, making up ~8% of total phospholipid. Site-specific phosphorylation of the phosphatidylinositol head group at distinct subcellular locations is an important cellular mechanism for targeting cytosolic proteins to specific membrane subdomains and is a crucial aspect of multiple signal transduction and vesicular transport pathways (1). PI 3-kinases are involved in the regulation of a broad range of processes including mitosis, cytoskeletal organization, apoptosis, and membrane trafficking (2, 3).

Metazoan cells possess three classes of PI 3-kinase. Class I enzymes phosphorylate PI 4-phosphate and PI 4,5-bisphosphate and are signaling PI 3-kinases acting primarily at the plasma membrane and activated, for example, by tyrosine phosphorylation following mitogenic stimulation or by heterotrimeric G-protein signaling (4, 5). Class II kinases are less well studied but have similar substrate specificity to class I enzymes and are also involved in signaling. Class II kinases may additionally function in clathrin-mediated endocytosis (6, 7). Class III PI 3-kinases are all related to the yeast vacuolar sorting protein Vps34p and, unlike the class I and II enzymes, appear to be universal across eukaryotic evolution (2, 8).

Class III PI 3-kinases mediate phosphorylation of PI to produce PI (3)P and have an evolutionarily conserved role in late endosomal transport. Yeast Vps34p regulates transport to the vacuole, whereas the human class III PI 3-kinase, hVPS34, is required for multivesicular body morphogenesis and for transport of lysosomal proteins (9–11). Class III PI 3-kinases have been implicated in a variety of processes, one of the best understood being their role as downstream effectors of the small GTPase, Rab5, in endosomal membrane fusion. The main site of PI (3)P production is at the endosomal membrane in mammalian cells, but high levels are also found in the lumen of the yeast vacuole (12). Yeast Vps34p exists in a complex with a myristoylated, WD40 domain-containing protein kinase, Vps15p (13). The mammalian homologue of Vps15p, adaptor protein p150, binds to the active, GTP-bound form of Rab5,

<sup>3</sup> The abbreviations used are: PI, phosphatidylinositol; BSA, bovine serum albumin; BSF, bloodstream form; ConA, concanavalin A; DAPI, 4'-6-Diamidino-2-phenylindole; FYVE, FAB1-YOTB-Vac1-EEA1; GFP, Green Fluorescent Protein; GPI, glycosylphosphatidylinositol; GRASP, Grp1 (general receptor for phosphoinositides-1)-associated scaffold protein; ORF, open reading frame; PBS, phosphate-buffered saline; RFP, red fluorescent protein; RNAi, RNA interference; VSG, variant surface glycoprotein; PI (3)P, phosphatidylinositol 3-phosphate; TGN, *trans*-Golgi network; FITC, fluorescein isothiocyanate; RT, reverse transcription.

targeting both protein and PI 3-kinase to early endosomes and leading to the Rab5-dependent generation of PI (3)P on endosomal membranes (14). Endosomal fusion in turn is promoted by the recruitment of the tethering factor EEA1, which binds to PI (3)P via a FYVE (FAB1-YOTB-Vac1-EEA1) domain (15, 16). EEA1 also interacts with numerous factors on both donor and acceptor membranes including Rab5 and syntaxins 6 and 13, allowing formation of oligomeric complexes that drive membrane fusion (17, 18). A similar process governs endosomal fusion in yeast, with Vac1p and Ypt31p taking the places of EEA1 and Rab5, respectively (19). Class III PI 3-kinases are not only required for vacuolar transport in yeast and multivesicular body formation in mammals but have also been implicated in the processes of retrograde endosome to *trans*-Golgi network (TGN) trafficking, via direct binding to retromer, and in autophagy (3, 20, 21). Additionally, in human cells hVPS34 interacts with Rab7 on late endosomes and is regulated by that GTPase (22). Overall, Vps34 has a multitude of functions and is a central coordinating factor of the endomembrane system.

The flagellated protozoan parasite *Trypanosoma brucei* has one of the better understood endomembrane systems among the highly divergent eukaryotes (23, 24). The mammalian infective bloodstream form (BSF) possesses a very active endocytic system responsible for maintenance of the protective variant surface glycoprotein (VSG) coat, uptake of nutrients, and removal of surface bound antibodies (24). The parasite is highly polarized, with all uptake and secretion restricted to an invagination at the base of the flagellum termed the flagellar pocket. Studies of VSG turnover have revealed an efficient recycling system in which all of the surface protein, receptor-bound, and fluid phase cargo are endocytosed via clathrin-coated vesicles and then sorted in a tubular endosome with the bulk of the VSG returning rapidly to the surface (25, 26). *T. brucei* expresses two Rab5 GTPases, TbRAB5A and TbRAB5B, which are associated with distinct cargos (27). Although these two proteins appear to have subtly distinct functions, both are essential for survival and are required for maintenance of endocytic function (28). No downstream effectors have been identified for either TbRAB5A or TbRAB5B, and their mechanisms of action are unknown. The presence of at least 12 FYVE domain proteins in the *T. brucei* genome, all with orthologues in other kinetoplastid genomes, suggests that PI (3)P production is important in the regulation of cellular functions in trypanosomatids. Here we describe the identification and functional analysis of TbVps34, the trypanosome orthologue of Vsp34; in particular we uncovered an unexpected role for TbVps34 in segregation of the Golgi apparatus at cytokinesis.

## MATERIALS AND METHODS

**Bioinformatics**—TbVps34 was identified by BLAST analysis by screening human and yeast PI 3-kinase protein sequences against the *T. brucei* data bases at GeneDB ([www.genedb.org](http://www.genedb.org)) and the TIGR *T. brucei* genome project ([www.tigr.org/tdb/mdb/tdb/](http://www.tigr.org/tdb/mdb/tdb/)). Orthology was confirmed by reverse BLAST. Alignments and phylogenetic analysis were performed between TbVps34 and Vps34-related sequences from NCBI and GeneDB using ClustalW.

**Cell Lines and Culture**—The tetracycline-inducible trypanosome cell line BSF 90–13 was routinely cultured in HMI-9 medium supplemented with 10% tetracycline-free fetal bovine serum (Autogen Bioclear). To maintain the tetracycline responsive phenotype cells were grown in the continuous presence of 5  $\mu\text{g/ml}$  hygromycin B and 2.5  $\mu\text{g/ml}$  geneticin (both from Sigma). The cells were maintained at concentrations between  $1 \times 10^4$  and  $2 \times 10^6 \text{ ml}^{-1}$ . For growth curves, triplicate cultures were initiated at  $1 \times 10^5 \text{ ml}^{-1}$  with or without tetracycline at a concentration of 1  $\mu\text{g ml}^{-1}$ . Cell concentration was determined using a Z2 Coulter counter (Beckman).

**Plasmids and Transfection**—A fragment of the TbVps34 sequence selected and verified by RNAi (29) was amplified by PCR with the primers CGGGATCCGGTTGCTGTTCAAAGTGGGT and GGAAGCTTGTGCCTCCACCATTTCCTTA and cloned into BamHI/HindIII-digested p2T7<sup>2Ti</sup> (gift of Doug LeCount). Tetracycline-responsive BSF 90–13 cells were transfected with NotI-digested p2T7<sup>2Ti</sup>·TbVps34 by electroporation, incubated for 6 h, and then selected for 1 week with 2.5  $\mu\text{g ml}^{-1}$  phleomycin. The cells were maintained thereafter in the presence of phleomycin. RNAi was induced by incubation with 1  $\mu\text{g ml}^{-1}$  tetracycline. GFP2xFYVE excised from pEGFP2xFYVE (gift from Harald Stenmark) was inserted into pHD1034 (gift of Christine Clayton) via HindIII/BamHI sites. pHD1034·RFP-GRASP was derived from pXS5·RFP-GRASP (originally a gift from Graham Warren). pHD1034 constructs were digested with NotI and transfected into p2T7<sup>2Ti</sup>·TbVps34 cells by electroporation. The cells were incubated for 6 h, then puromycin (0.1  $\mu\text{g ml}^{-1}$ ) was added, and the cells were selected for 1 week.

**Immunofluorescence**—For p67 immunofluorescence, the cells were fixed in 4% paraformaldehyde, adhered to poly-L-lysine slides (Sigma), and permeabilized with 0.1% Triton X-100. The slides were blocked with 10% goat serum in PBS. For staining of p67, the slides were incubated in monoclonal antibody 280 (gift of Jay Bangs) diluted in blocking buffer containing 0.02% sodium azide for 1 h at room temperature. For basal body and paraflagellar rod staining, the cells were air dried onto slides and fixed in methanol at  $-20^\circ\text{C}$ . The slides were blocked with 3% BSA in PBS and then incubated for 1 h with BBA4 or PFR-A monoclonal antibody in PBS/BSA (gift of Keith Gull). After washing with PBS, the slides were incubated with Oregon Green- or Texas Red-conjugated goat anti-mouse IgG (Molecular Probes) for 1 h at room temperature. The slides were washed and mounted with Vectashield containing DAPI (Vector Laboratories). The cells were examined under a Nikon Eclipse E600 microscope, and images were captured using a Photometrix Coolsnap FX camera and prepared with Adobe Photoshop 7.0.

**Fluid Phase Uptake**—Fluid phase uptake was monitored using Alexa Fluor 488 dextran 10000 (Molecular Probes) as described (30). Briefly, RNAi was induced by incubation for 18 h with 1  $\mu\text{g ml}^{-1}$  tetracycline, and the cells were harvested and resuspended at a concentration of  $1 \times 10^8 \text{ cells ml}^{-1}$  in 50  $\mu\text{l}$  of fresh medium. Labeled dextran was added to a concentration of 5  $\text{mg ml}^{-1}$ , and the cells were incubated for various times at  $37^\circ\text{C}$ . Uptake was stopped by the addition of 1 ml of

## PI3 Kinase Functions in Trypanosome Golgi Biogenesis

ice-cold HMI9 medium, and the cells were washed once at 4 °C before fixing for 1 h at 4 °C in 4% paraformaldehyde. The cells were adhered to slides, mounted, and examined immediately. The images were captured as described above. For quantitation, the images were taken under nonsaturating conditions using identical exposure times. Fluorescence intensity was determined using Metamorph Imaging software.

**Transferrin Uptake**—Uptake of FITC-transferrin (Molecular Probes) was performed as described (28). RNAi was induced for 18 h, and the cells were harvested and washed once in serum-free HMI9 medium containing 1% BSA. The cells were resuspended in HMI9/BSA at a concentration of  $1 \times 10^7$  ml<sup>-1</sup> and incubated at 37 °C for 20 min. FITC-transferrin (100 μg ml<sup>-1</sup>) was added, and the cells were incubated at 37 °C for various times. Uptake was stopped by the addition of 1 ml of ice-cold HMI9 medium, and the cells were washed once at 4 °C before fixing for 1 h at 4 °C in 4% paraformaldehyde. The cells were adhered to slides, mounted, and examined immediately. The images were captured and fluorescence intensity was quantified as described above.

**Uptake of Concanavalin A**—The cells were harvested and washed once in serum-free HMI9 medium containing 1% BSA. The cells were resuspended in HMI9/BSA at a concentration of  $1 \times 10^7$  ml<sup>-1</sup> and incubated at 4 °C or 37 °C for 20 min. Biotin or FITC-conjugated ConA (100 μg ml<sup>-1</sup>) (Vectalabs) was added, and the cells were incubated for a further 30 min. Uptake was stopped by placing the cells on ice. The labeled cells were washed in HMI9/BSA at 4 °C, then fixed with 4% paraformaldehyde for 1 h, and adhered to slides as described above. For p67 co-localization, the cells were permeabilized by incubation with 0.1% Triton X-100. For GFP2xFYVE co-localization, the cells were permeabilized with 0.05% saponin. The slides were blocked as described, and biotinylated ConA was detected by incubating for 1 h at room temperature with Texas Red-conjugated streptavidin (Vectalabs). The slides were either mounted immediately or counterstained with antibody as described.

**Wortmannin Treatment**—Cells expressing the GFP2xFYVE construct were incubated in liquid culture with wortmannin at a range of concentrations and times of exposure (0.01–30 μM and 30–120 min), and the location of the GFP construct was assessed after preparation for immunofluorescence as described above. Wortmannin stock was freshly prepared by dissolving the solid in dry Me<sub>2</sub>SO.

**Electron Microscopy**—For transmission electron microscopy, the cells were fixed in suspension by adding chilled 5% glutaraldehyde (TAAB) and 8% paraformaldehyde (Sigma) in PBS in a 1:1 ratio to the growth medium containing trypanosomes. The cells were fixed on ice for 10 min and centrifuged at 10,000 rpm for 5 min in 2-ml microcentrifuge tubes, and the supernatant was carefully replaced with fresh fixative for a further 50 min without disturbing the pellet, rinsed in 0.1 M sodium cacodylate, and post-fixed in 1% osmium tetroxide (TAAB) in same buffer at room temperature for 1 h. After rinsing in buffer, the cells were then dehydrated in an ethanol series, adding 1% uranyl acetate at the 30% stage, followed by propylene oxide, then embedded in Epon/Araldite 502 (TAAB), and finally polymerized at 60 °C for 48 h. Sections were cut on a Leica Ultracut T ultramicrotome at 70 nm using a diamond knife, contrasted

with uranyl acetate and lead citrate, and examined on a Philips CM100 transmission electron microscope.

**VSG Exocytosis**—Export was monitored as described (31). Briefly,  $5 \times 10^7$  mid-log phase BSF cells were washed once in labeling medium (Met/Cys-free Dulbecco's modified Eagle's medium (Sigma) supplemented with 10% dialyzed fetal calf serum and Hepes, pH 7.4), resuspended in 1 ml of labeling medium, and incubated at 37 °C for 15 min. The cells were pulse labeled at 37 °C for 7 min with Promix at a concentration of 200 μCi ml<sup>-1</sup>, then diluted 1:10 with prewarmed complete HMI9, and chased for up to 1 h at 37 °C. At intervals during the chase, aliquots of cells were removed from the sample and placed on ice. Following centrifugation in a microcentrifuge (20,000 × g at 4 °C), cell pellets were washed once in 1 ml of ice-cold PBS/1 mg ml<sup>-1</sup> BSA and resuspended in 920 μl of hypotonic lysis buffer. After 5 min on ice, the lysates were incubated at 37 °C for 10 min to enable GPI-specific phospholipase C to convert susceptible membrane form VSG to soluble VSG. The lysates were centrifuged for 10 min at 20,000 × g at 4 °C, and 900 μl of supernatant was retained. The pellet fraction was washed in ice-cold hypotonic lysis buffer, then resuspended in 1 ml of ice-cold sample lysis buffer, and incubated on ice for 25 min. 90 μl of 10× sample lysis buffer and 10 μl of Nonidet P-40 was added to the supernatant fraction to bring the buffers to equivalence. The lysates were clarified by centrifugation for 15 min (20,000 × g, 4 °C). Labeled VSG was recovered from the supernatants by incubation for 1 h at 4 °C with ConA-Sepharose 4B in the presence of 1 mM CaCl<sub>2</sub>, 1 mM MnCl<sub>2</sub>. After washing, the samples were resuspended in sample buffer and loaded onto 10% SDS-PAGE gels at  $1 \times 10^5$  cell equivalents/lane. Fixed, stained gels were treated for 1 h with Enhance (PerkinElmer Life Sciences) and autoradiographed. Image intensity was quantified using imageJ software.

**Semi-quantitative RT-PCR**—The Cells were incubated for 24 h in the presence or absence of 1 μg ml<sup>-1</sup> tetracycline then  $5 \times 10^7$  cells were harvested and washed once in PBS. RNA was extracted using TRIzol reagent (Invitrogen), precipitated with isopropanol, ethanol-washed, resuspended in diethyl cyanophosphonate-treated water, and stored at a concentration of 0.5–1 mg ml<sup>-1</sup> at –80 °C. Semi-quantitative RT-PCR was performed using the Titan One-Tube RT-PCR system (Roche Applied Science) (32). TbVps34 message was detected using the primers AACCGAATGGAACCTTGCCAC (forward) and CATAGCCGCTGTGTATCCCT (reverse), designed to amplify a segment of the TbVps34 gene distinct from the fragment used for RNAi. As a control, primers specific for α-tubulin, CAGAGAAGGCCTACCACGAG (forward) and CTCTTCCATACCCTGACCGA (reverse) were used. Assays for TbVps34 contained 400 ng of RNA, and those for α-tubulin contained 100 ng of RNA. For the reverse transcription step, the samples were incubated at 50 °C for 30 min and then at 94 °C for 2 min. For amplification, the samples were incubated at 94 °C for 30 s, 56 °C for 30 s, and 68 °C for 30 s for 30 cycles followed by a 7-min extension at 68 °C. Cycling conditions were optimized to ensure concentration dependence of amplification, and the absence of contaminating genomic DNA was confirmed by omission of the reverse transcription step (not shown). Similar results were obtained in duplicate experiments.

**Yeast Complementation**—The full-length TbVPS34 ORF was amplified by PCR with the following primers: forward TATTGAATTCATGGCCACGAACGAGGAC and reverse TATAC-TCGAGTGTGAGCCTTTAGGC, and inserted into EcoRI and XhoI sites in the pYES2Ct expression vector polylinker (2 $\mu$ , URA3; Invitrogen). The yeast Vps34 knockout strain, SEY6210  $\Delta$ vps34::TRP1 was transformed with empty vector pYES2Ct or pYES2CtTbVPS34. Yeast Vps34 PI 3-kinase complementation by TbVPS34 was confirmed by spotting serial dilutions of yeast cells, initially calibrated by optical density, carrying empty pYES2Ct vector or pYES2CtTbVPS34 on synthetic selective media plates (DO-TRP/URA). The plates were incubated for 4 days at 37 °C.

## RESULTS

**TbVps34 Is a Class III PI 3-Kinase**—The *T. brucei* genome data base GeneDB contains 14 open reading frames (ORFs) encoding proteins with predicted phosphatidylinositol kinase domains (see supplemental Table S1). Of these, eight show some level of homology to PI 3-kinases. However, the presence of FRAP, ATM, TRAPP/FRAP, ATM, TRRAP, C-terminal domain (FAT/FATC) accessory domains places six of these in the category of the target of rapamycin (TOR)-related atypical protein kinases, a family of protein kinases with lipid kinase-like catalytic domains that lack demonstrable ability to phosphorylate lipid substrates. Membership of this distinct subgroup is confirmed by phylogenetic analysis of the aligned proteins (supplemental Fig. S1A). Of the remaining two ORFs with a PI 3-kinase-like domain, one (Tb11.01.6980, accession number EAN80479) is an unusual kinase with a catalytic domain most similar to a PI 3-kinase combined with a PI (3)P-binding FYVE domain and a putative transmembrane sequence. However, the degree of conservation is relatively weak, sharing only 18% identity with mammalian PI 3-kinases in the kinase domain. Alignment suggests a closer homology to the atypical protein kinases than to genuine PI kinases (supplemental Fig. S1A). Therefore, this protein cannot be assigned with confidence to any particular PI kinase subfamily. Based on comparison of sequences, it seems likely that *T. brucei*, like yeast, possesses only one genuine PI 3-kinase, Tb927.8.6210 (accession number AAX69336), present as a single copy on chromosome eight.

The Tb927.8.6210 gene encodes a 949-amino acid protein with a very high level of homology to Vps34 by BLAST analysis against the nonredundant data base ( $p = 1.5e^{-87}$ ) (Fig. 1 and supplemental Fig. S1). Orthology was confirmed by reverse BLAST against *Homo sapiens* and *Saccharomyces cerevisiae* genome sequences. The TbVps34 protein sequence shares the Class III PI 3-kinase domain structure, with an N-terminal C2 domain (residues 109–252), an accessory domain (residues 357–547), and a C-terminal kinase domain (residues 694–891) (Fig. 1A). The catalytic domain shares 43% identity and 63% similarity with the human Vps34 homologue, but only 32% identity and 51% similarity with human Class II PI 3-kinase  $\alpha$ -chain. In particular, the activation loop sequence between residues 826 and 836 of TbVps34, which confers substrate specificity, indicates a Class III enzyme (33). Further, a critical lysine residue within the active site (Lys<sup>720</sup> in Tb927.8.6210 in supple-

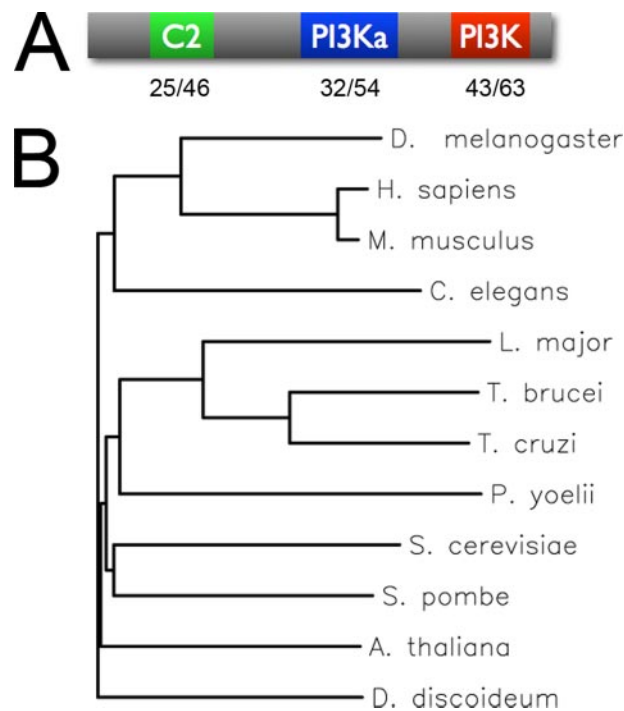
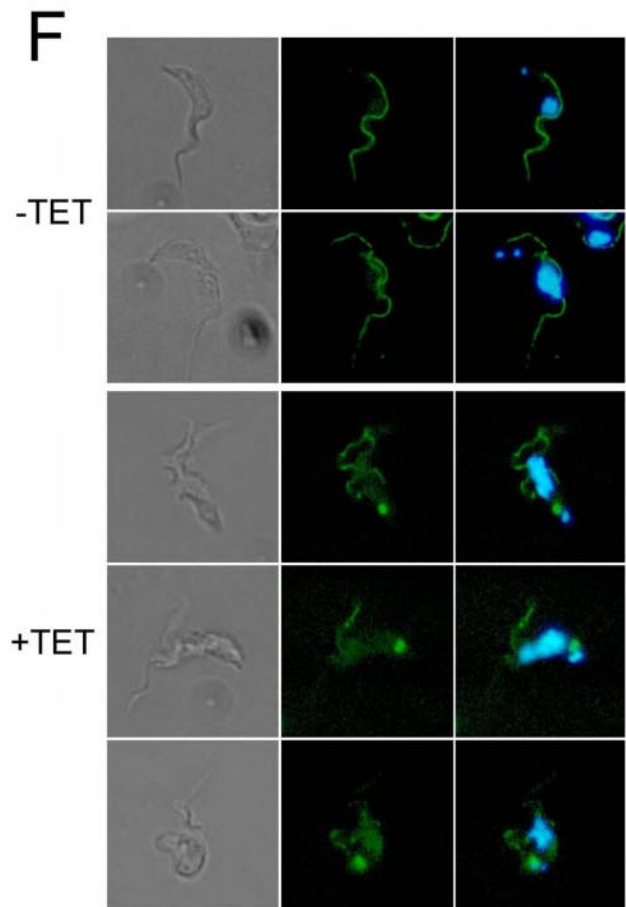
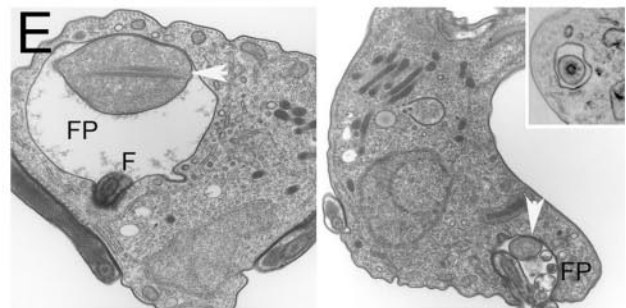
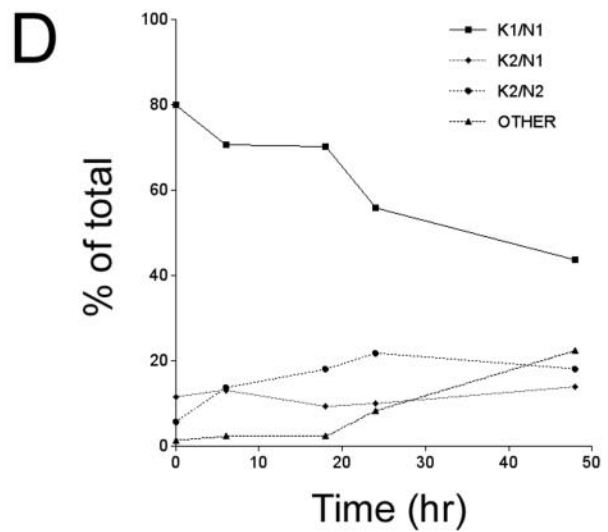
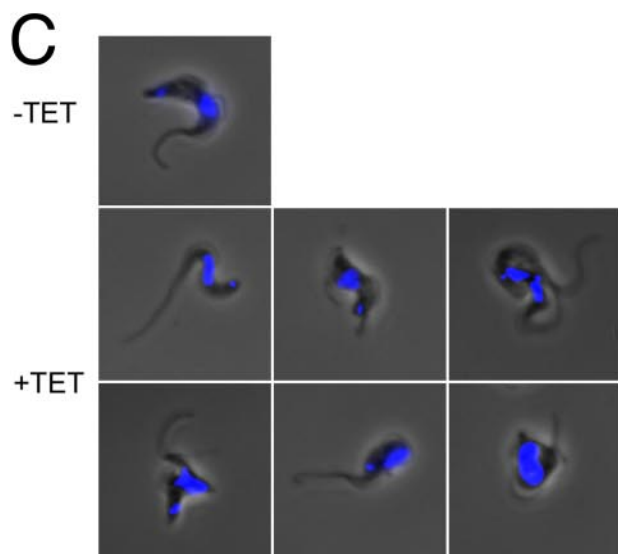
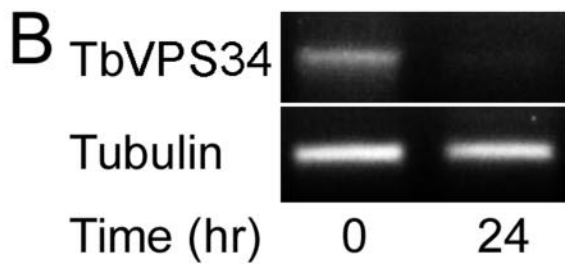
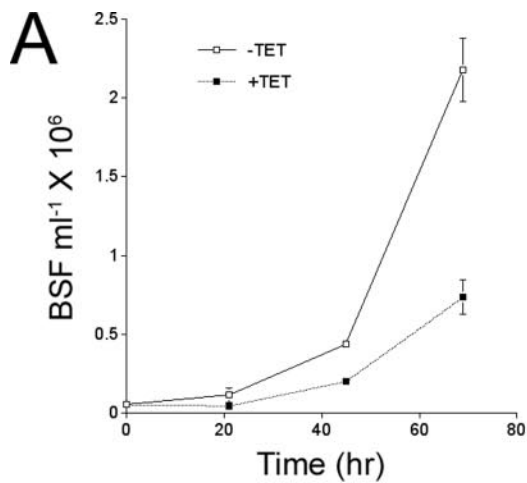


**FIGURE 1. TbVps34 is a Class III PI 3-kinase.** A, domain structure of the *T. brucei* Vps34 phosphatidylinositol kinase orthologue (TbVps34) identified by BLAST analysis of kinases against the Conserved Domain data base followed by ClustalW alignment. The numbers indicate percentages of identity and similarity to the human Class III PI 3-kinase orthologue for each domain as defined by ClustalW alignment (C2 in green, accessory domain in blue, and catalytic domain in red). B, phylogenetic tree of Class III PI 3-kinases based on ClustalW alignments using the neighbor-joining method with 1000 bootstraps.

mental Fig. S1B) that is essential for kinase activity and is covalently modified by wortmannin in mammalian PI 3-kinases is also conserved. Likewise the accessory and C2 domains are characteristic of Class III PI 3-kinases. The gene encoding the next closest homologue in *T. brucei*, Tb927.4.1140, lacks any obvious accessory domains, only shares a 30% identity with the hVPS34 kinase domain, and is more similar to a PI 4-kinase than a PI 3-kinase. Phylogenetic analysis shows that the *T. brucei* PI 3-kinase forms part of a protist-specific clade of Vps34-like genes from other kinetoplastid parasites (Fig. 1B) and indicates that the Vps34 family is present throughout the eukaryotes. Further, the major binding partner of Vps34p, Vps15p (or p150 in metazoa), which is required for function, can also be recovered from the *T. brucei* genome (Tb11.01.0930, accession number XM823891) and is orthologous to *S. cerevisiae* Vps15 by reverse BLAST (data not shown). Based on the sequence data, Tb927.8.6210 is most likely to be a lipid kinase that phosphorylates PI at position 3 to produce PI (3)P and to function in vesicle trafficking rather than signal transduction, and we propose that the product of Tb927.8.6210 be called TbVps34p.

**TbVps34 Is Required for Normal Growth of Bloodstream *T. brucei***—The function of TbVps34 was addressed using RNA interference. Tetracycline-inducible BSF cells were transfected with the RNAi plasmid p2T7Ti (34) containing a fragment of the TbVps34 gene. Induction of TbVps34 RNAi with tetracycline led to a rapid and profound inhibition of growth (Fig. 2A). Semi-quantitative RT-PCR showed an almost complete loss of

*PI3 Kinase Functions in Trypanosome Golgi Biogenesis*



TbVps34 expression by 24 h of induction, whereas tubulin levels remained constant (Fig. 2B). Light microscopic examination showed a variety of morphological abnormalities (Fig. 2C) that became more severe with increased time under RNAi. Examination of DAPI-stained slides revealed a progressive fall in the proportion of cells in S phase and an increase in cells with two nuclei and two kinetoplasts 24 h after induction (Fig. 2D). By 48 h abnormal cells with multiple nuclei or lacking either the nucleus or kinetoplast are common. This suggests that cells are able to progress through mitosis but are blocked in cytokinesis and also have organelle segregation defects.

Ultrastructural analysis of induced cells showed that enlargement of the flagellar pocket, a common feature of cells defective in endocytosis, is present in ~10% of induced cells (Fig. 2E). However, the effect is neither as pronounced nor as common as that in cells where endocytosis is specifically blocked (31). A more remarkable feature is the presence of vesicles and inclusions within the flagellar pocket, some of which contain paracrystalline material, similar in appearance to the paraflagellar rod (*arrows*). Staining of cells for the paraflagellar rod protein PFR-A showed that although uninduced cells have a uniform distribution of PFR-A along the length of the flagellum, there is an unusual accumulation of the protein within the flagellar pocket (Fig. 2F) in many induced cells. A similar pattern of staining was seen with anti-VSG antibodies (supplemental Fig. S3), indicating an unusual accumulation of both plasma membrane and flagellar proteins in the flagellar pocket. This is reminiscent of the membrane blebbing and microvesicle extrusion seen in kinetoplastids treated with drugs such as the lysolipid drug edelfosine, which is a known inhibitor of PI 3-kinase activity (35, 36). This distinctive phenotype was not inducible by RNAi of the other identified PI kinases of *T. brucei* (data not shown) and suggests multiple roles for TbVps34 in the maintenance of cell function.

*TbVps34 Is an Authentic PI 3-Kinase*—PI (3)P is present at extremely low levels in most cells, making direct measurement of PI 3-kinase activity in the trypanosome difficult, whereas expression of Vps34 polypeptides in bacteria usually results in insoluble and inactive protein. Therefore, we used several alternative approaches. First, we used the trypanosome Vps34 ORF to complement a *S. cerevisiae* Vps34 knockout strain, SEY6210Δ*vps34::TRP1*, that is temperature-sensitive for growth (68). Because Vps34p is the only PI 3-kinase present in *S. cerevisiae* and the lipid kinase activity of Vps34p is

required for function, this assay represents a highly stringent assessment of the ability of TbVps34p to act as a PI 3-kinase. Expression of TbVps34 from the pYES2 plasmid restored the ability of SEY6210Δ*vps34::TRP1* cells to grow at 37 °C, whereas transfection with the empty vector did not (Fig. 3), indicating that the TbVps34 gene product indeed possesses PI 3-kinase activity. Further, we directly addressed the effect of TbVps34 RNAi on cellular PI (3)P levels. The fluorescent probe GFP2xFYVE, containing GFP fused to a tandem repeat of the FYVE domain from the *H. sapiens* HRS protein, has been used to localize PI (3)P within the cell (12). This is a highly specific probe that is used widely and is the method of choice for monitoring PI (3)P production, especially in live or fixed cells (37). GFP2xFYVE only recognizes PI (3)P and does not interact with the inositol head group phosphorylated at positions 4 and 5 or with any of the multiply phosphorylated forms. In mammalian cells, the protein is targeted to the early endosome. By electron microscopy, 2xFYVE probes can be localized to the endosome and internal vesicles of multivesicular bodies in fibroblasts and are found primarily in the vacuole in yeast (12). When expressed in *T. brucei*, GFP2xFYVE is associated with compartments between the nucleus and flagellar pocket, consistent with an endosomal location (24) and which duplicates at mitosis (Fig. 3A). Overlap with endocytosed concanavalin A, under conditions that specifically label the flagellar pocket and lysosome (38), suggests that the majority of the GFP signal is associated with a late endosomal and/or lysosomal compartment (Fig. 3B).

We initially investigated PI (3)P production by inhibition of PI-kinases with wortmannin. This irreversible inhibitor covalently bonds to a critical conserved lysine residue within the active site of PI kinases (39) that is conserved in TbVps34. We required greater concentrations of wortmannin (3 μM) to perturb GFP2xFYVE location in trypanosomes than in mammalian cells (IC<sub>50</sub> = 4.2 nM for mammalian cells) but were able to obtain essentially complete loss of the GFP signal from permeabilized cells (Fig. 3). This suggests that the parasite protein, although still sensitive to the inhibitor, has a reduced sensitivity similar to that reported for yeast (IC<sub>50</sub> = 3 μM) (40). Apart from the modified lysine, the precise residues in the active site responsible for wortmannin binding and activity are not yet defined, making prediction of sensitivity difficult (41). These data indicate that the

**FIGURE 2. TbVps34 is required for normal growth and morphology.** *A*, TbVps34 RNAi inhibits growth. BSF 90–13 cells transfected with p2T7<sup>2Ti</sup>-TbVps34 were incubated with (*closed squares*) or without (*open squares*) 1 μg ml<sup>-1</sup> tetracycline (*TET*) to induce RNAi, and growth was monitored with a Coulter counter. Each point represents the mean of triplicate values ± S.D. This figure is typical of multiple experiments. *B*, loss of TbVps34 message in cells induced for RNAi. RNA was extracted from cells incubated in the presence or absence of 1 μg ml<sup>-1</sup> tetracycline for 24 h. TbVps34 and α-tubulin messages were amplified by RT-PCR as described under “Materials and Methods.” Control experiments omitting the RT confirmed the absence of contaminating genomic DNA (data not shown). Similar results were obtained in duplicate experiments. *C*, TbVps34 RNAi induces a variety of morphological abnormalities. p2T7<sup>2Ti</sup>-TbVps34 cells were incubated in the presence (+*TET*) or absence (-*TET*) of 1 μg ml<sup>-1</sup> tetracycline for 24 h. The cells were harvested, fixed with 4% paraformaldehyde, and stained with DAPI to show the location of the nucleus and kinetoplast. *D*, TbVps34 RNAi causes a block in cytokinesis. p2T7<sup>2Ti</sup>-TbVps34 cells were induced for various times with 1 μg ml<sup>-1</sup> tetracycline then fixed and stained with DAPI as described above. Kinetoplast/nucleus ratios were determined for at least 100 cells for each time point analyzed. Similar results were obtained in duplicate assays. *K*, kinetoplast; *N*, nucleus. *OTHER* includes zoids (cytoplasts lacking a nucleus), akinetoplast cells, cells with grossly distorted nuclei containing more than a diploid copy of the genome, and cells with three or more nuclei. *E*, disruption of the flagellar pocket induced by TbVps34 RNAi. Electron micrographs of p2T7<sup>2Ti</sup>-TbVps34 BSF induced with tetracycline for 24 h. Note the enlarged flagellar pocket in the *left panel* and inclusions in the flagellar pocket in *both panels* (*arrowheads*). The *inset* shows a transverse section through the flagellar pocket and flagellar axoneme of a control bloodstream stage cell for reference. *F*, flagellum; *FP*, flagellar pocket. *F*, accumulation of PFR-A in the flagellar pocket of cells induced for TbVps34 RNAi. Immunofluorescence of cells incubated for 24 h with (+*TET*) or without (-*TET*) 1 μg ml<sup>-1</sup> tetracycline before fixation with methanol at -20 °C. The cells were stained with monoclonal antibody against PFR-A (*green*) as described under “Materials and Methods” and counterstained with DAPI (*blue*).

## PI3 Kinase Functions in Trypanosome Golgi Biogenesis

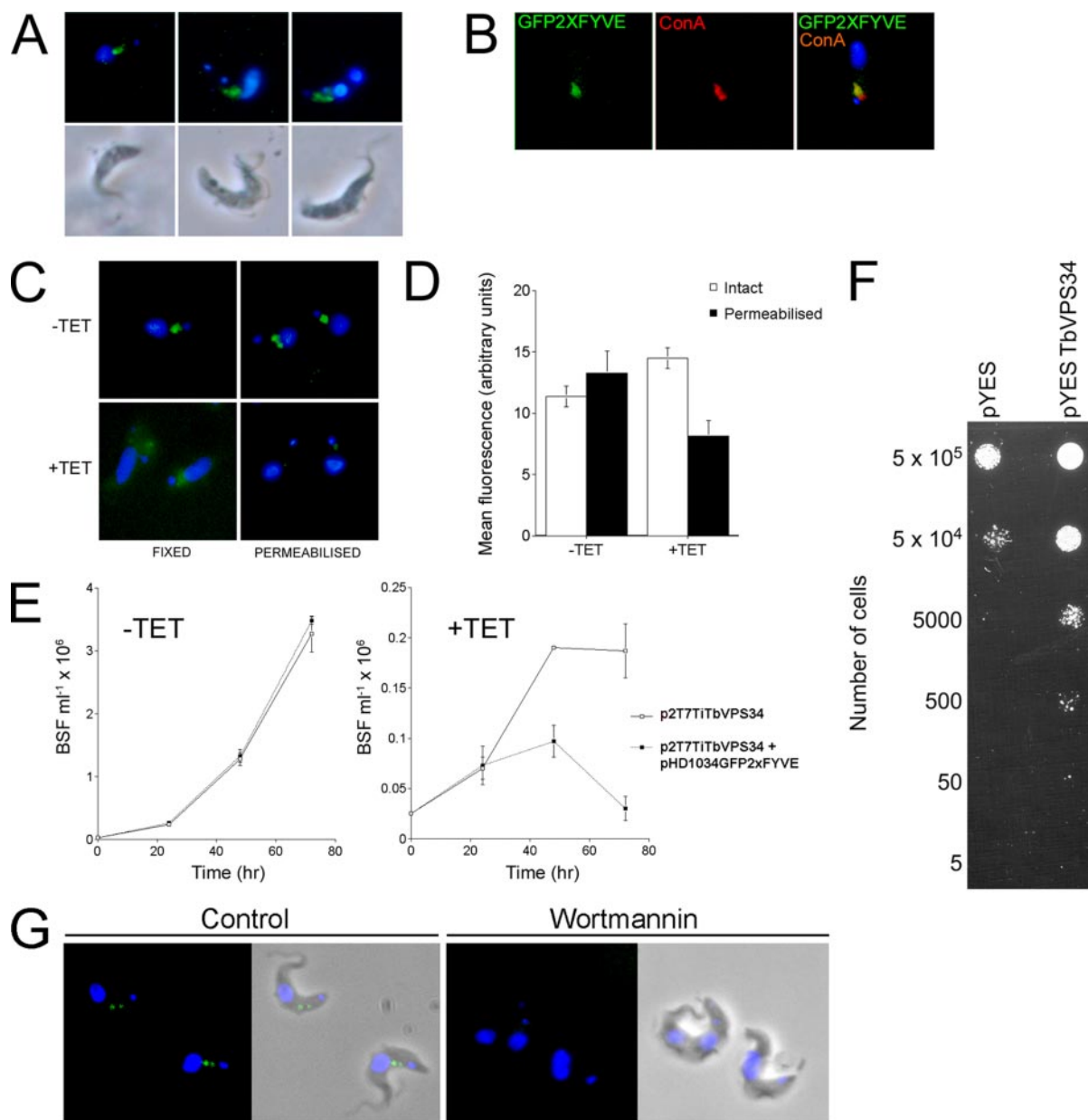


**FIGURE 3. Biosynthesis of PI (3)P by TbVps34.** *A*, localization of GFP2xFYVE in uninduced cells. p2T7<sup>2T1</sup>·TbVps34 cells co-transfected with pHD1034 containing the PI (3)P probe GFP2xFYVE were fixed with 4% paraformaldehyde and stained with DAPI. The images were captured at various stages of the cell cycle. *B*, GFP2xFYVE co-localizes with endocytosed ConA. Uninduced cells were allowed to accumulate biotinylated ConA for 30 min, permeabilized with 0.05% saponin, stained with Texas Red-streptavidin, and counterstained with DAPI. *C*, GFP2xFYVE disperses after induction of TbVps34 RNAi. The cells were incubated in the absence (–TET) or presence (+TET) of 1  $\mu\text{g ml}^{-1}$  tetracycline for 24 h. The cells were either fixed (left panels) or fixed and permeabilized with saponin (right panels). *D*, quantitative loss of GFP2xFYVE staining in permeabilized cells after induction of TbVps34 RNAi. Mean cellular fluorescence for fixed (open bars) or permeabilized (closed bars) cells incubated with or without tetracycline for 24 h. Each bar represents the mean value for at least 30 cells  $\pm$  S.E. Similar results were obtained in triplicate experiments. The loss of fluorescence in the permeabilized cells is extremely significant ( $p < 0.0001$ , unpaired  $t$  test). *E*, expression of GFP2xFYVE enhances the growth inhibitory effect of TbVps34 RNAi. Growth curves for parental p2T7<sup>2T1</sup>·TbVps34 cells (open squares) and cells also expressing GFP2xFYVE (closed squares) incubated in the presence (+TET) or absence (–TET) of 1  $\mu\text{g ml}^{-1}$  tetracycline. Each point represents the mean of triplicate counts  $\pm$  S.D. Similar results were obtained in duplicate experiments. *F*, TbVps34 rescues the growth defect of a *S. cerevisiae* Vps34 knockout. The full-length TbVps34 ORF was amplified by PCR and inserted into EcoRI and XhoI sites in pYES2Ct and verified by direct DNA sequencing. The *S. cerevisiae* Vps34 knockout, SEY6210  $\Delta\text{vps34}::\text{TRP1}$  is temperature-sensitive for growth, exhibiting a severe growth defect at 37 °C (68). The SEY6210 $\Delta\text{vps34}::\text{TRP1}$  yeast strain (kind gift of Dr. Y. Ohsumi, Okazaki, Japan) was transformed with empty vector, pYES2Ct, or pYES2Ct:TbVps34. Serial dilutions of cells carrying empty vector or expressing TbVps34 were spotted onto selective plates and grown for 96 h at 37 °C as indicated. The severe growth impairment observed in the SEY6210 $\Delta\text{vps34}::\text{TRP1}$  cells was rescued by expression of full-length TbVps34, indicating that *T. brucei* Vps34 is able to complement *S. cerevisiae* Vps34 and confirming the gene product as possessing authentic PI 3-kinase activity. *G*, inhibition of phosphatidylinositol phosphate synthesis in trypanosomes by wortmannin perturbs GFP2xFYVE localization. Trypanosomes expressing GFP2xFYVE were cultured in the presence (left) or absence (right) of wortmannin (3  $\mu\text{M}$ , 60 min, 37 °C) and then fixed, permeabilized, and processed for microscopy. Essentially complete delocalization and loss of the GFP signal (green) is observed in the wortmannin-treated cells, highly similar to the alterations observed with the TbVps34 knockdown (compare with Fig. 3C). The cells were counter-stained with DAPI (blue) to mark the nucleus and kinetoplast, and images are shown overlaid with phase in the right panel of each pair. These data confirm the assignment of function for TbVps34 as a PI kinase made on the basis of primary structure and also that the localization of GFP2xFYVE is dependent on ongoing phosphoinositide synthesis in trypanosomes. Note that the concentration and time of exposure to wortmannin was systematically tested, and the concentration used was the minimum dose that produced a clear effect on GFP2xFYVE localization.

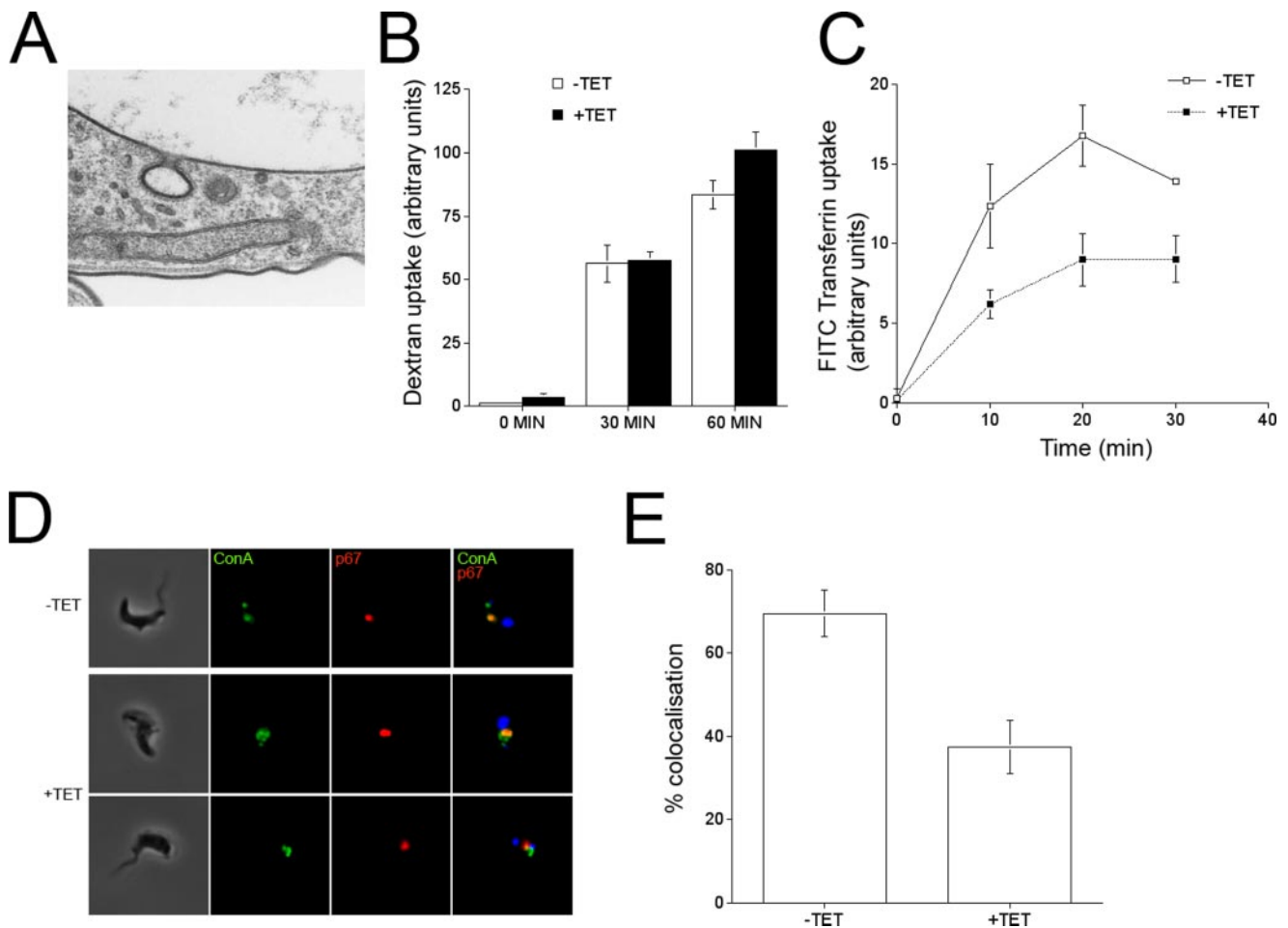


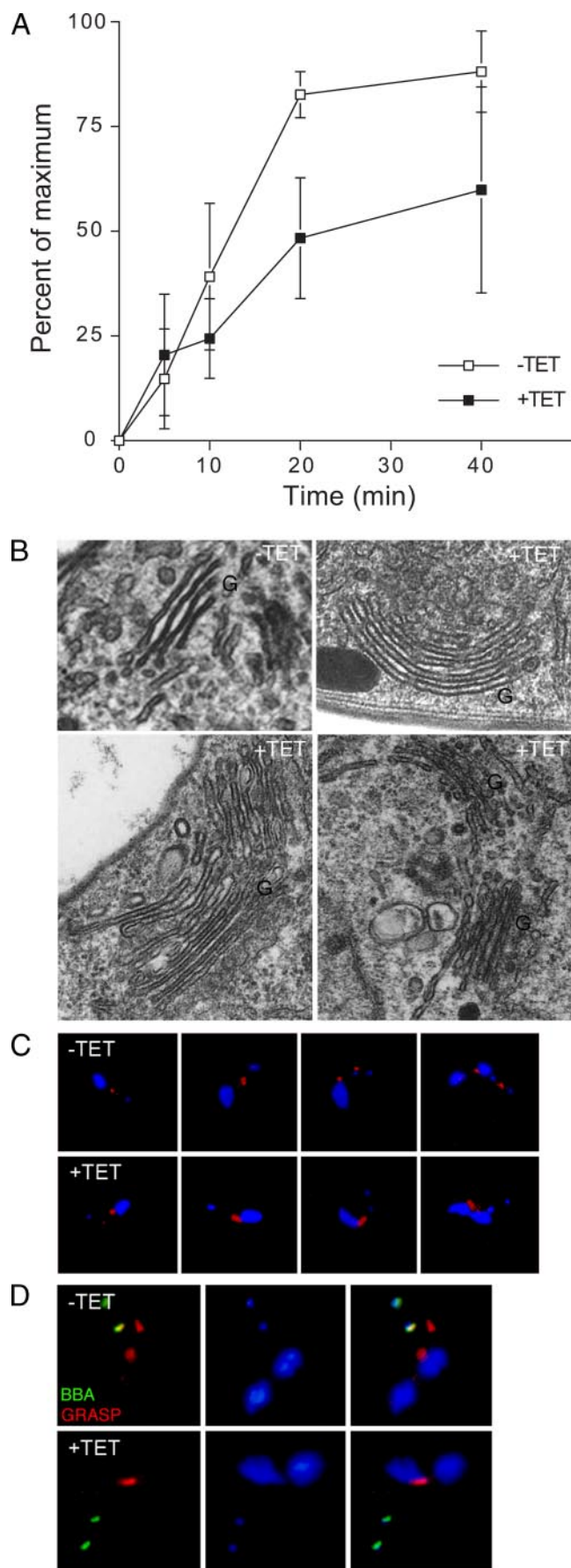
**FIGURE 4. TbVps34 RNAi reduces receptor-mediated uptake of transferrin but not fluid phase endocytosis.** *A*, TbVps34 RNAi does not prevent formation of clathrin-coated pits. Electron micrograph of a p2T7<sup>2T1</sup>-TbVps34 BSF cell after 24 h induction with tetracycline, showing a clathrin-coated pit budding from the flagellar pocket membrane. Budding vesicles were apparent in many of the cells examined. *B*, fluid phase uptake is unaffected by TbVps34 RNAi. Endocytosis of Alexa Fluor 488 dextran 10000 in p2T7<sup>2T1</sup>-TbVps34 cells incubated in the absence (*open bars*) and presence (*closed bars*) of tetracycline for 18 h was measured by quantitative fluorescence microscopy as described under "Materials and Methods." The values represent the mean fluorescence for at least 30 cells  $\pm$  S.E. The result is representative of triplicate assays. *C*, inhibition of transferrin uptake by TbVps34 RNAi. Accumulation of FITC-transferrin in p2T7<sup>2T1</sup>-TbVps34 cells incubated in the absence (*open squares*) and presence (*closed squares*) of tetracycline for 18 h, quantitated by microscopy as described under "Materials and Methods." Each point represents the mean fluorescence for at least 30 cells  $\pm$  S.E. Similar results were obtained in triplicate assays. *D*, transport of FITC-ConA to the lysosome is impaired in TbVps34 RNAi. Cells incubated for 24 h in the presence (+TET) or absence (-TET) of 1  $\mu$ g ml<sup>-1</sup> were labeled with FITC-ConA (*green*) for 30 min at 37 °C and counterstained with monoclonal antibody 280 against the lysosomal protein p67 (*red*). Note the high degree of co-localization in control cells compared with induced cells. *E*, quantitation of degree of overlap between p67 and ConA using Metamorph Imaging Software. Each bar represents the mean co-localization for at least 10 cells  $\pm$  S.E. Similar results were obtained in multiple experiments.

localization of GFP2xFYVE in trypanosomes requires ongoing PI (3)P synthesis.

To further validate TbVps34 as a PI 3-kinase, p2T7<sup>2T1</sup>-TbVps34 cells were co-transfected with the constitutive expression plasmid pHD1034 containing GFP2xFYVE. On induction of TbVps34 RNAi, the location of GFP2xFYVE became more dispersed (Fig. 3C). Permeabilization and washing of uninduced cells has little effect on cellular GFP levels, indicating stable association of the GFP with internal membranes, but led to a significant fall in GFP fluorescence in induced cells ( $p < 0.01$ ), indicating more efficient extraction of the GFP in the induced line, suggesting a reduction in PI (3)P caused by a loss of TbVps34 activity (Fig. 3D). Because PI (3)P is a comparatively polar lipid, bearing two phosphates in the head group, preferential extraction by mild detergent treatment is to be expected. This pattern of loss of GFP2xFYVE detection in saponin-treated cells is also seen in mammalian cells treated

with wortmannin (12). The failure to completely abolish GFP2xFYVE localization in some cells suggests that some residual PI (3)P is present and is probably a reflection of variable efficiency of the RNAi.

Expression of the 2xFYVE constructs can lead to alterations in endosomal structure, and high levels compete with EEA1 for endosomal binding sites (12). To determine whether the probe was having any effect on the *T. brucei* BSF, growth rates were monitored. Uninduced p2T7<sup>2T1</sup>-TbVps34 cells expressing GFP2xFYVE show similar growth patterns to the parental line, suggesting that the effect of the probe is minimal in normal cells (Fig. 3E). Significantly, when TbVps34 RNAi was induced with tetracycline, the presence of GFP2xFYVE increased the severity of the RNAi growth defect. A higher level of abnormal and dead cells was seen in affected cultures, reflected in the fall in cell number after prolonged induction. This increased sensitivity to RNAi suggests a synthetic interaction between GFP2xFYVE



and TbVps34 that is probably the result of increased competition for binding sites between the probe and endogenous FYVE domain proteins as PI (3)P levels become limited. Taken together these observations confirm that TbVps34 is a class III PI 3-kinase; moreover, the nearly complete loss of GFP2xFYVE membrane localization is also consistent with TbVps34 as the only major PI 3-kinase activity in the trypanosome.

**TbVps34 RNAi Interferes with Receptor-mediated Transport in BSF Trypanosomes**—Although some cells induced for TbVps34 RNAi exhibit enlargement of the flagellar pocket (Fig. 2E), clathrin-coated vesicles budding from the pocket are clearly visible in the majority of cells examined by electron microscopy (Fig. 4A), showing that the early stages of endocytosis remain functional. To determine whether loss of TbVps34 is involved in later stages of the endocytic pathway, fluid phase uptake of dextran and receptor-mediated endocytosis of transferrin were examined by fluorescent microscopy. Uptake of the fluid phase marker, Alexa Fluor 488 dextran 10000, is unaffected by induction of TbVps34 RNAi (Fig. 4B), but accumulation of transferrin was partially blocked (Fig. 4C). Fluid phase and membrane-bound cargo are taken up into the cell together but are rapidly sorted into distinct compartments. Most transferrin entering the cell is rapidly recycled from the early endosome (42), but a proportion is transported to the late endosome/lysosome (43). To determine whether TbVps34 regulates intracellular transport of surface-bound proteins to terminal endocytic compartments, the cells were labeled with FITC-Concanavalin A and co-stained for the lysosomal marker p67 (44) (Fig. 4D). In untreated cells, some concanavalin A can be seen at the flagellar pocket, but most co-localizes with p67. After induction of TbVps34 RNAi, co-localization with p67 is significantly reduced (Fig. 4E). These results confirm a specific role for TbVps34 in the later stages of receptor-mediated endocytosis.

**TbVps34 RNAi Blocks VSG Export**—In *S. cerevisiae*, in addition to its role in vacuolar transport, Vps34p regulates retrograde traffic from the endosome to the TGN, and indeed a proportion of Vps34p/Vps15p complex is located at the yeast TGN. To determine whether TbVps34 has any function in the trypanosome secretory pathway, the effect of TbVps34 RNAi on the export of the major surface protein VSG was monitored.

**FIGURE 5. TbVps34 RNAi interferes with VSG export and Golgi segregation.** **A**, p2T7<sup>2Ti</sup>-TbVps34 cells were incubated for 24 h in the presence or absence of 1  $\mu\text{g ml}^{-1}$  tetracycline. VSG export in <sup>35</sup>S pulse-labeled cells was monitored by the appearance over time of soluble VSG in hypotonic lysates incubated at 37 °C to allow GPI-phospholipase C-dependent cleavage of the GPI anchor (45). VSG was isolated from solubilized pellet and supernatant fractions and separated on a 12% SDS-PAGE gel. The percentage of VSG label in supernatant and pellet fractions was quantitated from autoradiographs using NIH Image at each time point. The intensity of bands was measured using ImageJ software. **B**, electron micrographs of p2T7<sup>2Ti</sup>-TbVps34 BSF induced with tetracycline for 24 h. Note the extended Golgi stacks in induced cells. G, Golgi. **C**, failure of Golgi segregation in cells lacking TbVps34 expression. p2T7<sup>2Ti</sup>-TbVps34 cells were transfected with pHD1034-RFP-GRASP as a probe for the Golgi. The cells were incubated for 24 h with (+TET) or without (-TET) 1  $\mu\text{g ml}^{-1}$  tetracycline, methanol-fixed, and stained with DAPI. The images were taken of cells at different stages of the cell cycle. Note that two Golgi stacks are apparent in uninduced cells at later stages of the cycle, but only one is detected in induced cells. **D**, TbVps34 RNAi does not affect basal body duplication and segregation. The cells co-transfected with p2T7<sup>2Ti</sup>-TbVps34 and pHD1034-RFP-GRASP were induced for 24 h with 1  $\mu\text{g ml}^{-1}$  tetracycline, methanol-fixed, and stained with the anti-basal body antibody BBA4 (green). The cells were counterstained with DAPI.

The cells were pulsed with  $^{35}\text{S}$ , and the acquisition of sensitivity to endogenous GPI-specific phospholipase C was used as an indicator of translocation to the surface (Ref. 45; see Ref. 31 for a detailed validation of this method) (Fig. 5A). The data demonstrate that in uninduced cells the majority of VSG is exported to the plasma membrane with a half-time of approximately 10 min, but in cells induced for TbVps34 RNAi, a marked proportion of labeled VSG fails to reach the surface during the time of the experiment. Thus secretory export is impaired when TbVps34 expression is modulated.

**Uncoupling of Golgi and Basal Body Segregation in TbVps34 RNAi**—The inhibition of VSG export suggests an important role for TbVps34 and thus PI (3)P in the secretory pathway. Electron microscopy revealed that many TbVps34-RNAi-induced cells possess an unusually extended Golgi apparatus, with an increase to both the number and length of the cisterna within the stacks (Fig. 5B). To examine the effect of TbVps34 RNAi on the Golgi in more detail, the cells were transfected with pHD1034 carrying RFP-GRASP, a fusion of RFP with the full-length TbGRASP, the trypanosome homologue of the mammalian Golgi matrix protein GRASP55 (46). As expected, the RFP fusion protein can be clearly seen localized to a single perinuclear site in uninduced S phase cells (Fig. 5C, *first panel*). As previously reported, RFP-GRASP could also be found at the basal body in some cells (47), but detection of non-Golgi-associated GRASP was highly variable in our hands. The Golgi duplicates in parallel with the kinetoplast prior to nuclear division, and the new Golgi segregates with the daughter nucleus after nuclear division (48). However, after induction of TbVps34 RNAi, although the Golgi appears to duplicate normally, as demonstrated by an elongated Golgi spot with a central constriction, complete segregation fails to take place, even though kinetoplast and nuclear division appear to progress unimpaired (Fig. 5C, *lower panels*). In untreated cells, 85% of 2K2N cells contained clearly segregated Golgi ( $n = 52$ ). By contrast, 71% of induced cells at this stage of the cycle possessed a single, enlarged Golgi ( $n = 58$ ). Similar results were obtained in duplicate experiments. Further, a similar defect was also observed in cells treated with wortmannin under the conditions established for inhibition of PI (3)P synthesis; although 100% of untreated cells with a 2K1N organelle content had two distinct RFP-GRASP spots ( $n = 25$ ), only 58% had separated the Golgi complex following 1 h of exposure to the inhibitor ( $n = 50$ ). The lower frequency of the wortmannin block to Golgi segregation compared with the RNAi is likely due to the much shorter exposure time for the former condition. In addition, this effect on RFP-GRASP localization was not seen in knockdown of a closely related PI 4-kinase-like protein (Fig. S3), suggesting that the effect of both TbVps34 and wortmannin treatment was specifically due to the loss of PI (3)P.

The position of the trypanosome Golgi complex is dictated by the basal body, with the distance between the Golgi and basal body maintained constant throughout the cell cycle (47). We noticed that the position of the RFP-GRASP staining in cells that had failed to segregate the Golgi complex was slightly altered, and the Golgi appeared closer to the nucleus than in normal cells, suggesting a potential perturbation of the Golgi-basal body relationship (Fig. 5, C and D; compare positions of

the nucleus and kinetoplast with Fig. 3, A and G). To determine whether the failure of cells lacking TbVps34 to segregate the Golgi properly was due to an effect on the basal body, RFP-GRASP-expressing cells were stained with the anti-basal body monoclonal antibody BBA4 (Fig. 5D). Basal body location and duplication both appear to be unaffected by TbVps34 RNAi. Thus the processes of Golgi and basal body segregation are uncoupled by interference with PI 3-kinase activity. These observations suggest a novel function for phosphatidylinositol kinases in the control of organelle positioning during cell division and imply that the block in cytokinesis associated with TbVps34 RNAi is the result of a failure of the Golgi to partition correctly during mitosis.

## DISCUSSION

Primary structural analysis places the TbVps34 gene product as a Class III PI 3-kinase, and based on the effects following knockdown by RNAi, TbVps34 clearly shares with its mammalian and *S. cerevisiae* orthologues a central role in vesicular trafficking and endocytosis. Furthermore, complementation of the yeast Vps34 and specific ablation of membrane association of a PI (3)P-specific probe, GFP2xFYVE, confirms TbVps34 as a PI 3-kinase and also indicates that it is the major, if not only, enzyme responsible for PI (3)P generation in trypanosomes. The lack of a potent effect of TbVps34 RNAi on the earliest stages of endocytosis, combined with the lysosomal location of PI (3)P in the trypanosome, indicate that TbVps34 activity is likely most important for the later stages of endocytosis and specifically in the transport of cargo taken up by receptor-mediated endocytosis to the lysosome, similar to yeast (49). The observation that fluid phase endocytosis is apparently unaffected by TbVps34 RNAi is similar to the situation described for mammalian cells, where bulk endocytic transport was not blocked by inhibition of PI 3-kinase activity, but sorting of the EGF receptor was impaired (50). The involvement of TbVps34 in trafficking to the lysosome thus mirrors the function of Vps34p in both mammalian and yeast systems (9, 10).

TbVps34 is the only gene encoding a classic PI 3-kinase-like protein in the *T. brucei* genome. Like *S. cerevisiae*, *T. brucei* does not appear to possess any class I or class II PI 3-kinase genes, and therefore it is unlikely that trypanosomes use PI 3-kinase-dependent signaling pathways. However, the genome does include a number of protein kinases possessing the phosphoinositide-binding pleckstrin homology, phox, and FYVE domains (51, 52).<sup>4</sup> None of these kinases has a clearly defined function at present, although one, ZFK, is involved in regulation of differentiation (52). Several additional and novel FYVE domain proteins are also encoded by the trypanosome genome, including a small Ras-like GTPase (53). Thus it remains possible that TbVps34 contributes to signal transduction by regulating the localization of protein kinase activity or by a truly trypanosome-specific mechanism.

The distinctive morphological effects of TbVps34 RNAi, particularly the changes in the flagellar pocket, are not found in cells blocked at different points of the endocytic and secretory pathways by knockdown of Rab proteins or other

<sup>4</sup> B. S. Hall and M. C. Field, unpublished observations.

## PI3 Kinase Functions in Trypanosome Golgi Biogenesis

essential regulators of vesicular traffic (28, 30, 31, 54) and thus suggest that the kinase may play a wider role in the control of cell organization. The precise mechanism by which PFR components become preferentially incorporated into these flagellar pocket-located membrane-bounded structures is not known, nor is it known whether there is involvement of the flagellar pocket in the normal trafficking of PFR components to the flagellum. However, the potential that the inhibition of PI (3)P production perturbs normal flagellar morphogenesis and that the vesicles represent an abortive attempt to construct a new flagellum, cannot be discounted. Under such a model, extrusion of a flagellar membrane without the full complement of internal components (*i.e.* axoneme and PFR) could then result in vesiculation of the membrane, to generate the structures seen here. Recapitulation of such a phenotype with edelfosine, a PI 3-kinase inhibitor, in *Leishmania* is also consistent with this model and suggests a potential role for PI (3)P in flagellar biogenesis, most likely intraflagellar transport (35, 36). This would also be consistent with the effects on cytokinesis and the accumulation of abnormal karyotypes in TbVps34 RNAi cultures because the flagellum is required for the correct completion of cell division. Present data cannot completely rule out an alternative possibility, that a vesicle blebbing pathway described in other kinetoplastids has become activated via the depletion of PI (3)P (35, 36). The inhibition of VSG export suggests potentially an additional role for TbVps34 in the secretory pathway, likely post-endoplasmic reticulum transport. However, an alternate explanation, that this is also a result of the defective flagellar targeting, is also possible.

There is much evidence to support a role for Class III PI 3-kinases in Golgi function in other systems. *S. cerevisiae* Vps34p and its mammalian orthologue regulate retrograde transport from the endosome to the TGN (20, 55). The PI (3)P-binding phox domain of sorting nexin 1 is implicated in this process (56), and the presence of genes for similar proteins in the *T. brucei* genome suggests this pathway may also function within kinetoplastids.<sup>4</sup> In addition, in higher eukaryotes PI (3)P is detectable at Golgi membranes, and some FYVE proteins are resident in the Golgi complex rather than associating with endosomal membranes (57), whereas the Vps15/p150 adaptor protein is also located at the TGN. Furthermore, a complex of Vps34p and Beclin involved in autophagy is primarily located to the Golgi (58). A number of studies using the inhibitor wortmannin also indicate a function for PI 3-kinases in maintenance of the Golgi complex, but interpretation is complicated by the ability of this drug to block the activity of other PI kinases involved in secretory transport (59, 60). In this study, using the GFP2x FYVE probe, we demonstrate that the majority of PI (3)P is located on endosomal membranes, but the presence of an additional, but lower abundance, pool on the Golgi complex cannot be eliminated.

The effect of TbVps34 RNAi on the Golgi complex during cell division was more unexpected. In budding yeast, Vps34p null mutants exhibit defective vacuolar segregation, and targeting of cargo from the Golgi to the vacuole is affected (9, 49), but no direct influence on the Golgi has been reported. It is possible

that in mammalian cells there are similar defects to those observed here; for example wortmannin perturbs interactions between the Golgi complex and the actin cytoskeleton in Rat RBL-2H3 cells (61) and also leads to hypertrophy of the Golgi cisternae (62), but the architecture of the trypanosome Golgi complex makes morphological alterations more easily observed compared with the extended Golgi ribbon in mammalian cells where such effects may not be apparent. In *T. brucei* the Golgi duplicates early in the cell cycle, in parallel with endoplasmic reticulum export sites, the material for the new Golgi being derived partly from the endoplasmic reticulum export site and partly from the old Golgi complex (47, 48). Duplication is closely linked to the replication of the basal body, the trypanosome equivalent of the centrosome, and a constant spatial relationship between Golgi complex and basal body is maintained even in the presence of inhibitors of nuclear division (47, 48). The mechanisms underlying these processes are unknown but are assumed to involve microtubules. Significantly, when TbVps34 expression is suppressed, the connection between basal body and Golgi complex replication and positioning is lost, whereas the Golgi complex also becomes localized rather closer to the nucleus than in untreated cells. Significantly, both ultrastructural and fluorescent microscopy data show that Golgi duplication proceeds normally, whereas the temporal association with basal body and kinetoplast division appears to be maintained. Thus the requirement for TbVps34 activity is most likely restricted to a specific post-replication point in the cell cycle when the two post-mitotic Golgi complexes separate. The role of TbVps34 in coordinating Golgi segregation may involve PI (3)P-dependent targeting of proteins to the Golgi, to the basal body or to the microtubular network, and a detailed analysis of phosphoinositide binding proteins will be needed to distinguish between these possibilities. TbVps34 may also act by a more indirect route. Several lines of evidence point to a role for Vps34-like enzymes in the nucleus, with suggested roles in transcription and telomere length regulation (3, 63). Thus TbVps34 may have other functions in addition to its role in vesicular transport.

The observations of TbVps34 function in cytokinesis are important for several reasons. First, the specific block in Golgi segregation points to a novel role for PI 3-kinases in control of organelle partitioning. Second, the data demonstrate that separation of the duplicated Golgi can be uncoupled from separation of the kinetoplast and basal body and also nuclear division. Finally, although cell division can proceed in the absence of nuclear separation, producing cytoplasts (64), correct partitioning of the Golgi appears to be necessary for the completion of cytokinesis. Segregation of organelles between daughter cells is tightly controlled in *T. brucei* and is necessary for maintenance of the protective VSG coat. The parasite may therefore have evolved mechanisms to ensure that cells cannot divide if the old and new Golgi complexes are not correctly separated, and daughter cells lacking a Golgi complex were not observed in either wortmannin or TbVps34-RNAi cultures. Interestingly, suppression of VSG expression by RNAi also results in a block to cell cycle progression (65); potentially a blockade to VSG exocytosis may explain the growth cessation obtained with the TbVps34 RNAi. However, as both experimental

approaches likely result in significant perturbation to biosynthetic trafficking through the endomembrane system, it is possible that VSG and TbVps34 RNAi activate the same or similar signaling pathways. A further explanation, that suppression of VSG expression in some manner affects Golgi (or other) organelle segregation, also cannot be ruled out based on the present data.

Our work and that of others has demonstrated that the maintenance of trafficking systems is vital to the survival of *T. brucei* BSF, but no obvious drug targets have been identified in the endocytic and secretory pathways. The interaction between Rab5 and both class I and class III PI3-kinases is well documented, as is the involvement of numerous FYVE domain containing proteins (including EEA1, rabankyrin5, and rabenosyn5) in Rab5 function. Recently it was found that Rab5 interacts with specific phosphatases capable of generating PI (3)P from higher order phosphatidylinositol polyphosphates, indicating that Rab5 acts to coordinate a complex network of activities for local generation of PI (3)P on membrane microdomains (66). Further, inhibitors of PI 3-kinase activity are of interest in the development of treatments against several conditions including cancer (67). In trypanosomes a PI 3-kinase is required for normal growth, indicating that this family of proteins may also be a potential target for anti-trypanosomal drugs. Similarities between TbVps34 RNAi and the actions of edelfosine suggest that some anti-kinetoplastid agents already under investigation may act at least in part through inhibition of PI kinase activity (35). PI kinase family proteins thus represent a promising direction for the identification of new trypanocides.

*Acknowledgments*—We thank the following for reagents: Keith Gull (University of Oxford) for BBA4 and PFR-A antibodies, Jay Bangs (University of Madison) for monoclonal antibody 280, Harald Stenmark (Norwegian Radium Hospital) for pEGFP2xFYVE, Christine Clayton (University of Heidelberg) for pHD1034, Graham Warren (Yale University) for RFP-GRASP, Helen Price (University of York) for pHD1034RFP-GRASP, and Yoshinori Ohsumi, (National Institute for Basic Biology, Okazaki, Japan) for *S. cerevisiae* strain SEY6210  $\Delta$ vps34::TRP1. We are also grateful to Keith Gull for discussion of the flagellum phenotype and suggestions as to its origin.

REFERENCES

1. Roth, M. G. (2004) **84**, 699–730
2. Foster, F. M., Traer, C. J., Abraham, S. M., and Fry, M. J. (2003) *J. Cell Sci.* **116**, 3037–3040
3. Rog, O., Smolikov, S., Krauskop, A., and Kupiec, M. (2005) *Curr. Genet.* **47**, 18–28
4. Auger, K. R., Serunian, L. A., Soltoff, S. P., Libby, P., and Cantley, L. C. (1989) *Cell* **57**, 167–175
5. Stoyanov, B., Volinia, S., Hanck, T., Rubio, I., Loubtchenkov, M., Malek, D., Stoyanova, S., Vanhaesebroeck, B., Dhand, R., Nurnberg, B., Gierschik, P., Seedorf, K., Hsuan, J. J., Waterfield, M. D., and Wetzker, R. (1995) *Science* **269**, 690–693
6. Brown, R. A., and Shepherd, P. R. (2001) *Biochem. Soc. Trans.* **29**, 535–537
7. Gaidarov, I., Smith, M. E., Domin, J., and Keen, J. H. (2001) *Mol. Cell.* **7**, 443–449
8. Field, M. C., Gabernet-Castello, C., and Dacks, J. B. (2006) in *Evolution of the Eukaryotic Endomembrane System and Cytoskeleton* (Jékely, G., ed) Landes/Eurekah Bioscience Publishers, Georgetown, TX
9. Herman, P. K., and Emr, S. D. (1990) *Mol. Cell. Biol.* **10**, 6742–6754

10. Brown, W. J., DeWald, D. B., Emr, S. D., Plutner, H., and Balch, W. E. (1995) *J. Cell Biol.* **130**, 781–796
11. Fernandez-Borja, M., Wubboltsm, R., Calafat, J., Janssen, H., Divecha, N., Dusseljee, S., and Neeffjes, J. (1999) *Curr. Biol.* **9**, 55–58
12. Gillooly, D. J., Morrow, I. C., Lindsay, M., Gould, R., Bryant, N. J., Gaullier, J. M., Parton, R. G., and Stenmark, H. (2000) *EMBO J.* **19**, 4577–4588
13. Stack, J. H., Herman, P. K., Schu, P. V., and Emr, S. D. (1993) *EMBO J.* **12**, 2195–2204
14. Christoforidis, S., Miaczynska, M., Ashman, K., Wilm, M., Zhao, L., Yip, S. C., Waterfield, M. D., Backer, J. M., and Zerial, M. (1999) *Nat. Cell Biol.* **1**, 249–252
15. Gaullier, J. M., Simonsen, A., D'Arrigo, A., Bremnes, B., Stenmark, H., and Aasland, R. (1998) *Nature* **394**, 432–433
16. Simonsen, A., Lippe, R., Christoforidis, S., Gaullier, J. M., Brech, A., Callaghan, J., Toh, B. H., Murphy, C., Zerial, M., and Stenmark, H. (1998) *Nature* **394**, 494–498
17. McBride, H. M., Rybin, V., Murphy, C., Giner, A., Teasdale, R., and Zerial, M. (1999) *Cell* **98**, 377–386
18. Simonsen, A., Gaullier, J. M., D'Arrigo, A., and Stenmark, H. (1999) *J. Biol. Chem.* **274**, 28857–28860
19. Peterson, M. R., Burd, C. G., and Emr, S. D. (1999) *Curr. Biol.* **9**, 159–162
20. Burda, P., Padilla, S. M., Sarkar, S., and Emr, S. D. (2002) *J. Cell Sci.* **115**, 3889–3900
21. Petiot, A., Ogier-Denis, E., Blommaert, E. F., Meijer, A. J., and Codogno, P. (2000) *J. Biol. Chem.* **275**, 992–998
22. Stein, M. P., Feng, Y., Cooper, K. L., Welford, A. M., and Wandinger-Ness, A. (2003) *Traffic* **4**, 754–771
23. Berriman, M., Ghedin, E., Hertz-Fowler, C., Blandin, G., Renauld, H., Bartholomeu, D. C., Lennard, N. J., Caler, E., Hamlin, N. E., Haas, B., et al. (2005) *Science* **309**, 416–422
24. Morgan, G. W., Hall, B. S., Denny, P. W., Carrington, M., and Field, M. C. (2002) *Trends Parasitol.* **18**, 491–496
25. Grunfelder, C. G., Engstler, M., Weise, F., Schwarz, H., Stierhof, Y. D., Morgan, G. M., Field, M. C., and Overath, P. (2003) *Mol. Biol. Cell.* **14**, 2029–2040
26. Engstler, M., Thilo, L., Weise, F., Grunfelder, C., Schwarz, H., and Boshart, M. (2004) *J. Cell Sci.* **17**, 1105–1115
27. Pal, A., Hall, B. S., Nesbeth, D. N., Field, H. L., and Field, M. C. (2002) *J. Biol. Chem.* **277**, 9529–9539
28. Hall, B. S., Allen, C. L., Goulding, D., and Field, M. C. (2004) *Mol. Biochem. Parasitol.* **138**, 67–77
29. Redmond, S., Vadivelu, J., and Field, M. C. (2003) *Mol. Biochem. Parasitol.* **128**, 115–118
30. Hall, B. S., Smith, E., Langer, W., Jacobs, L. A., Goulding, D., and Field, M. C. (2005) *Eukaryot. Cell* **4**, 971–980
31. Allen, C. L., Goulding, D., and Field, M. C. (2003) *EMBO J.* **22**, 4991–5002
32. Marone, M., Mozzetti, S., De Ritis, D., Pierelli, L., and Scambia, G. (2001) *Biol. Proced. Online* **3**, 19–25
33. Pirola, L., Zvelebil, M. J., Bulgarelli-Leva, G., Van Obberghen, E., Waterfield, M. D., and Wymann, M. P. (2001) *J. Biol. Chem.* **276**, 21544–21554
34. LaCount, D. J., Bruse, S., Hill, K. L., and Donelson, J. E. (2000) *Mol. Biochem. Parasitol.* **111**, 67–76
35. Santa-Rita, R. M., Henriques-Pons, A., Barbosa, H. S., and de Castro, S. L. (2004) *J. Antimicrob. Chemotherapy* **54**, 704–710
36. Berggren, M. I., Gallegos, A., Dressler, L. A., Modest, E. J., and Powis, G. (1993) *Cancer Res.* **53**, 4297–4302
37. Carlton, J. G., and Cullen, P. J. (2005) *Trends Cell Biol.* **15**, 540–547
38. Brickman, M. J., Cook, J. M., and Balber, A. E. (1995) *J. Cell Sci.* **108**, 3611–3621
39. Wymann, M. P., Zvelebil, M., and Laffargue, M. (2003) *Trends Pharmacol Sci.* **24**, 366–376
40. Stack, J. H., and Emr, S. D. (1994) *J. Biol. Chem.* **269**, 31552–31562
41. Walker, E. H., Pacold, M. E., Perisic, O., Stephens, L., Hawkins, P. T., Wymann, M. P., and Williams, R. L. (2000) *Mol. Cell* **6**, 909–919
42. Pal, A., Hall, B. S., Jeffries, T., and Field, M. C. (2003) *Biochem. J.* **374**, 443–451
43. Grab, D. J., Wells, C. W., Shaw, M. K., Webster, P., and Russo, D. C. (1992) *Eur J. Cell Biol.* **59**, 398–404

## PI3 Kinase Functions in Trypanosome Golgi Biogenesis

44. Kelley, R. J., Brickman, M. J., and Balber, A. E. (1995) *Mol. Biochem. Parasitol.* **74**, 167–178
45. Ferguson, M. A., Duszenko, M., Lamont, G. S., Overath, P., and Cross, G. A. (1986) *J. Biol. Chem.* **261**, 356–362
46. Shorter, J., Watson, R., Giannakou, M. E., Clarke, M., Warren, G., and Barr, F. A. (1999) *EMBO J.* **18**, 4949–4960
47. He, C. Y., Ho, H. H., Malsam, J., Chalouni, C., West, C. M., Ullu, E., Toomre, D., and Warren, G. (2004) *J. Cell Biol.* **165**, 313–321
48. Field, H., Sherwin, T., Smith, A. C., Gull, K., and Field, M. C. (2000) *Mol. Biochem. Parasitol.* **106**, 21–35
49. Simonsen, A., Wurmser, A. E., Emr, S. D., and Stenmark, H. (2001) *Curr. Opin. Cell Biol.* **13**, 485–492
50. Petiot, A., Faure, J., Stenmark, H., and Gruenberg, J. (2003) *J. Cell Biol.* **162**, 971–979
51. Gale, M., Jr., and Parsons, M. (1993) *Mol. Biochem. Parasitol.* **59**, 111–121
52. Vassella, E., Kramer, R., Turner, C. M., Wankell, M., Modes, C., van den Bogaard, M., and Boshart, M. (2001) *Mol. Microbiol.* **41**, 33–46
53. Field, M. C. (2005) *Trends Parasitol.* **21**, 447–450
54. Hall, B. S., Pal, A., Goulding, D., and Field, M. C. (2004) *J. Biol. Chem.* **279**, 45047–45056
55. Hirosako, K., Imasato, H., Hirota, Y., Kuronita, T., Masuyama, N., Nishioka, M., Umeda, A., Fujita, H., Himeno, M., and Tanaka, Y. (2004) *Biochem. Biophys. Res. Commun.* **316**, 845–852
56. Carlton, J., Bujny, M., Peter, B. J., Oorschot, V. M., Rutherford, A., Mellor, H., Klumperman, J., McMahon, H. T., and Cullen, P. J. (2004) *Curr. Biol.* **14**, 1791–1800
57. Cheung, P. C., Trinkle-Mulcahy, L., Cohen, P., and Lucocq, J. M. (2001) *Biochem. J.* **355**, 113–121
58. Kihara, A., Kabeya, Y., Ohsumi, Y., and Yoshimori, T. (2004) *EMBO Rep.* **2**, 330–335
59. Domin, J., Gaidarov, I., Smith, M. E., Keen, J. H., and Waterfield, M. D. (2000) *J. Biol. Chem.* **275**, 11943–11950
60. Walch-Solimena, C., and Novick, P. (1999) *Nat. Cell Biol.* **1**, 523–525
61. di Campli, A., Valderrama, F., Babia, T., De Matteis, M. A., Luini, A., and Egea, G. (1999) *Cell Motil. Cytoskeleton* **43**, 334–348
62. Thyberg, J. (1998) *Eur. J. Cell Biol.* **76**, 33–42
63. Bunney, T. D., Watkins, P. A., Beven, A. F., Shaw, P. J., Hernandez, L. E., Lomonosoff, G. P., Shanks, M., Peart, J., and Drobak, B. K. (2000) *Plant Cell* **12**, 1679–1688
64. Robinson, D. R., Sherwin, T., Ploubidou, A., Byard, E. H., and Gull, K. (1995) *J. Cell Biol.* **128**, 1163–1172
65. Shearer, K., Vaughan, S., Minchin, J., Hughes, K., Gull, K., and Rudenko, G. (2005) *Proc. Natl. Acad. Sci. U. S. A.* **102**, 8716–8721
66. Shin, H. W., Hayashi, M., Christoforidis, S., Lacas-Gervais, S., Hoepfner, S., Wenk, M. R., Modregger, J., Uttenweiler-Joseph, S., Wilm, M., Nystuen, A., Frankel, W. N., Solimena, M., De Camilli, P., and Zerial, M. (2005) *J. Cell Biol.* **170**, 607–618
67. Wetzker, R., and Rommel, C. (2004) *Curr. Pharm. Des.* **10**, 1915–1922
68. Kihara, A., Noda, T., Ishihara, N., and Ohsumi, Y. (2001) *J. Cell Biol.* **152**, 519–530